

Dynamic evolution control for the DC/DC boost converter design and implementation

Ahmad Saudi Samosir, Sri Ratna Sulistiyanti, Herri Gusmedi, Luthfiyyatun Mardiyah

Department of Electrical Engineering, Faculty of Engineering, Universitas Lampung, Bandar Lampung, Indonesia

Article Info

Article history:

Received Aug 20, 2023

Revised Sep 6, 2023

Accepted Sep 28, 2023

Keywords:

Boost converter

Duty cycle formula

Dynamic evolution control

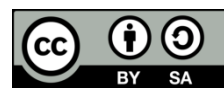
Hardware implementation

Non-linear controller

ABSTRACT

This paper introduces the design and hardware implementation of the dynamic evolution control for a DC/DC boost converter. The development of the controller aims to effectively regulate the output voltage of the DC/DC boost converter with a high degree of precision. A comprehensive examination of the duty cycle formula for the boost converter is conducted using a non-linear analysis approach. This study introduces a methodology for the synthesis of a converter controller utilizing the principles of dynamic evolution control theory. The converter's output consistently aligns with the target voltage by following the dynamic evolution path determined by the designed controller. The performance evaluation of the proposed boost converter controller utilizing dynamic evolution control is being validated through the utilization of MATLAB/Simulink simulation software. The effectiveness of the proposed controller is further validated through the presentation of hardware results. The performance of the controller was evaluated by varying the values of parameters k and m .

This is an open access article under the [CC BY-SA](https://creativecommons.org/licenses/by-sa/4.0/) license.



Corresponding Author:

Ahmad Saudi Samosir

Department of Electrical Engineering, Faculty of Engineering, Universitas Lampung

Soemantri Brojonegoro Street, Bandar Lampung, Indonesia

Email: saudi.ahmad@gmail.com

1. INTRODUCTION

The DC/DC power converter is widely researched and extensively employed in the field of power electronics. The utilization spectrum of DC/DC power converters encompasses various applications such as high-efficiency power supplies [1], [2], high-efficiency battery chargers [3], high voltage gain converters [4], [5], high-efficiency DC motor drives [6], [7], maximum power point tracking (MPPT) applications [8]–[10], and renewable energy conversion systems [11]–[14]. DC-DC converters are frequently employed in the context of inverter systems within photovoltaic systems [15]–[17], alongside wind turbines and other sources of renewable energy. Numerous scientists and researchers have conducted extensive studies and made significant advancements in the field of DC-DC converter designs, with the primary objective of attaining optimal power efficiency and performance [18]–[20].

The boost converter, a widely used DC-DC converter, is favored for its ability to increase voltage output from lower sources, making it suitable for powering high-voltage loads. This converter employs active switching components like MOSFETs and diodes, along with passive energy storage components such as inductors and capacitors, making it a non-linear second-order system [21]. However, it has a drawback related to closed-loop instability due to a zero in the model's right half plane, challenging voltage regulation. Researchers have been actively exploring control methods to address this issue.

Recent research highlights key findings: Yuan and Kim [22] introduces a compensated active disturbance rejection technique. Regulating boost converter output voltage can be achieved using State-

Feedback linearization or the Linear Quadratic regulator, both offering quick recovery, minimal steady-state error, and effective disturbance rejection.

In the operation of the boost converter, the presence of a dependable controller is imperative. This controller must possess the capability to modify the pulse width modulation (PWM) signal in order to generate a duty cycle that is suitable for achieving a stable output voltage and rapid response. The selection of an appropriate control method is crucial in ensuring the optimal performance of the boost converter. A variety of controllers have been developed to achieve high-performance and high-power efficiency. These controllers include proportional integral derivative (PID) controllers [23], [24], sliding mode controls (SMC) [25]–[28], internal model controls (IMC) [29], [30], dynamic evolution controls (DEC) [19], and various other adaptive control methods.

This paper discusses the application of dynamic evolution control (DEC) in improving the boost converter's control system. DEC is a novel method rooted in dynamic evolution theory that simplifies the synthesis of the duty cycle formula influencing pulse width modulation (PWM) signals. This approach addresses control issues by using a dynamic evolution model to generate control signals systematically. To design the converter controller, it employs a straightforward analysis of the nonlinear converter model.

The paper also demonstrates the implementation of a DEC controller to regulate the boost converter's output voltage. The effectiveness of this controller is verified through MATLAB/Simulink simulations, and the design and manufacturing processes of the hardware controller are detailed. Hardware results are presented to further validate the proposed controller's performance. The implementation employs the ATmega 328P microcontroller, and the controller's performance is evaluated by adjusting the parameter values of k and m , considering varying input voltage conditions.

2. METHOD

2.1. Analysis of DC-DC boost converter system

A boost converter, commonly referred to as a step-up converter, is a power electronics converter designed to raise the output voltage level from a lower DC voltage input. The primary components of a Boost Converter's main circuit include two static switches, typically a power MOSFET and a fast recovery diode, as well as two energy storage elements, comprising a power inductor and an electrolyte capacitor. Figure 1 illustrates a schematic diagram of the boost converter circuit. The operation of the boost converter can be dissected into two distinct operating modes known as the switch ON and OFF state, as depicted in Figure 2.

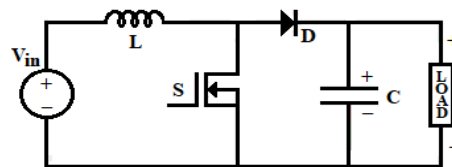


Figure 1. Boost converter's circuit diagram

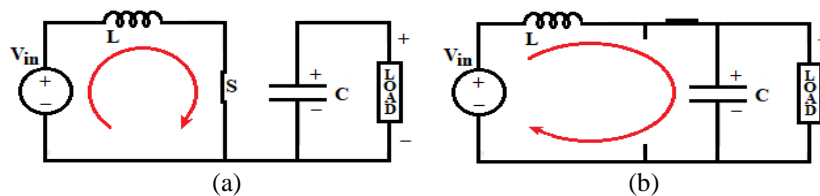


Figure 2. Operation mode of boost converter (a) ON state and (b) OFF state

When the switch ON state, as illustrated in Figure 2(a), it establishes a closed loop connecting the input voltage V_{in} to the inductor, causing a linear increase in inductor current. Simultaneously, the diode remains reverse-biased, effectively acting as an open switch, creating isolation between the load circuit and the power source. Consequently, in this mode, the load voltage is determined by the capacitor voltage, and the application of Kirchhoff's voltage law to the circuit diagram yields in (1) and (2).

$$L \frac{di_L}{dt} - V_{in} = 0 \quad (1)$$

$$V_{in} = L \frac{di_L}{dt} \quad (2)$$

When the switch OFF state, as depicted in Figure 2(b), it connects the input voltage V_{in} to the inductor and the diode. The diode becomes forward biased, establishing a connection between the input voltage V_{in} , the inductor, the capacitor, and the load. Consequently, the current originating from the input voltage flows towards the load. The inductor serves as a conduit for transferring the energy previously stored during the switch-ON phase to the load, resulting in a linear decrease in inductor current. Applying the Kirchhoff's voltage law to the circuit shown in Figure 2(b) yields in (3) and (4).

$$L \frac{di_L}{dt} + V_C - V_{in} = 0 \quad (3)$$

$$V_{in} = L \frac{di_L}{dt} + V_C \quad (4)$$

Utilizing the switching average model, with due consideration to the time intervals during which the switch is ON and OFF, we can formulate the voltage equation for the DC-DC boost converter based on (2) and (4) as follows, denoted as (5).

$$V_{in} = L \frac{di_L}{dt} + (1 - D) \cdot V_C \quad (5)$$

Because of the output voltage of the boost converter is parallelly connected to the output capacitor, it becomes possible to replace the capacitor voltage with the output voltage. Consequently, we can express the output voltage of the boost converter as follows:

$$V_O = \frac{1}{(1-D)} \left(V_{in} - L \frac{di_L}{dt} \right) \quad (6)$$

2.2. Synthesis of dynamic evolution control for the boost converter

The dynamic evolution control (DEC) technique is based on the principles of feedback control, which aims to actively respond to disturbances and minimize the difference between the system output and the set point input. DEC focuses on rapidly reducing any error state (the difference between output and reference input) to zero, emphasizing dynamic error state control. It achieves this by guiding the error state along a predefined path known as the evolution path, ensuring that the error state diminishes to zero over time [19].

In designing a controller with dynamic evolution control, the first step involves defining an evolution path to quickly reduce the error state to zero. By selecting an exponential function in Figure 3(a) as the evolution path, the system's dynamic characteristic value decreases exponentially to zero, as expressed by (7), and typical output voltage would be as Figure 3(b).

$$Y = C \cdot e^{-mt} \quad (7)$$

Here, Y represents the system's dynamic characteristic, C is the initial value of Y , and m is a design parameter determining the speed of evolution. When Y represents the dynamic function of a converter with an initial value Y_0 , in (8) shows how Y decreases exponentially towards zero with a decreasing rate m .

$$Y = Y_0 \cdot e^{-mt} \quad (8)$$

From (8), the dynamic evolution function can be written as (9) [19].

$$\frac{dY}{dt} + m \cdot Y = 0, \quad m > 0 \quad (9)$$

The synthesis process is carried out to create a control equation that ensures the system's dynamic characteristics reach zero by following the dynamic evolution path [19]. In the case of a DC-DC boost converter controller, this control equation is associated to the converter's duty cycle equation. The synthesis process initiates by defining the dynamic function Y . With Y is designated as the error voltage,

$$Y = k \cdot V_{err}(t) \quad (10)$$

Where k is a positive coefficient, and V_{err} is the error voltage which is the difference between the reference voltage and the output voltage. Using Y as defined in (10), the dynamic evolution function can be expressed as (11).

$$k \cdot \frac{dV_{err}(t)}{dt} + m \cdot k \cdot V_{err}(t) = 0 \quad (11)$$

On the other hand, the boost converter's output in (6) can be written as (12).

$$V_o(t) = V_{dc}(t) - L \frac{di_L(t)}{dt} + V_o(t) \cdot d(t) \quad (12)$$

By combining both sides of the output equation for the boost converter in (12) with (11), yields:

$$k \cdot \frac{dV_{err}(t)}{dt} + m \cdot k \cdot V_{err}(t) + V_o(t) = V_{dc}(t) - L \frac{di_L(t)}{dt} + V_o(t) \cdot d(t) \quad (13)$$

From (13), the equation for the PWM duty cycle can be derived as (14).

$$d(t) = \frac{k \cdot \frac{dV_{err}(t)}{dt} + m \cdot k \cdot V_{err}(t) + V_o(t) - V_{dc}(t) + L \frac{di_L(t)}{dt}}{V_o(t)} \quad (14)$$

The duty cycle in (14) forces the error state function ($Y=k \cdot V_{err}$) to follow the dynamic evolution function (9). As a result, as time goes by, the error state function ($Y=k \cdot V_{err}$) is forced to decrease progressively towards zero ($k \cdot V_{err} = 0$) at a decreasing rate m .

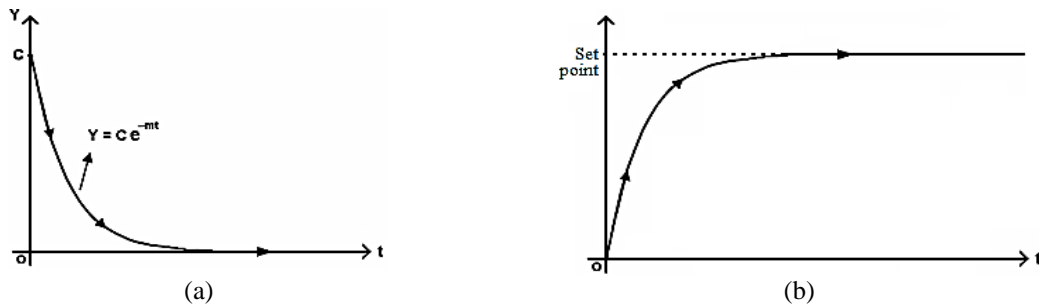


Figure 3. Dynamic evolution path and typical output voltage for (a) exponential evolution path and (b) typical output voltage

3. RESULT AND DISCUSSION

3.1. Simulation result

A comprehensive simulation was conducted to assess the dynamic evolution controller's performance in regulating the boost converter. This analysis utilized MATLAB/Simulink and was based on the model derived from (14). The model of boost converter controlled with dynamic evolution control and the dynamic evolution controller model are shown in Figure 4 and Figure 5 respectively. Their parameters are listed in Table 1.

Table 1. Parameters of simulation model

Parameters	Value	Unit
Voltage reference	25	V
Input voltage	12, 16, 20	V
Inductor inductance	1.2	mH
Capacitor (C)	470	μ F
Load 1 resistance	20	ohm
Load 2 resistance	10	ohm
Switching frequency	31.25	kHz

Figure 6 displays the simulation results of the boost converter's output voltage when V_{in} is set at 12 V. With a reference voltage of 25 V, the controllers effectively maintain the output voltage at 25 V. With this scenario, the duty cycle is estimated as $D = (V_{ref} - V_{in})/V_{ref}$, amounts to 52%. The output current, computed as $I_o = V_o/R$, equals 1.25 A. Consequently, the input current can be calculated using formula $I_{in} = I_o / (1 - D)$, resulting in 2.60 A.

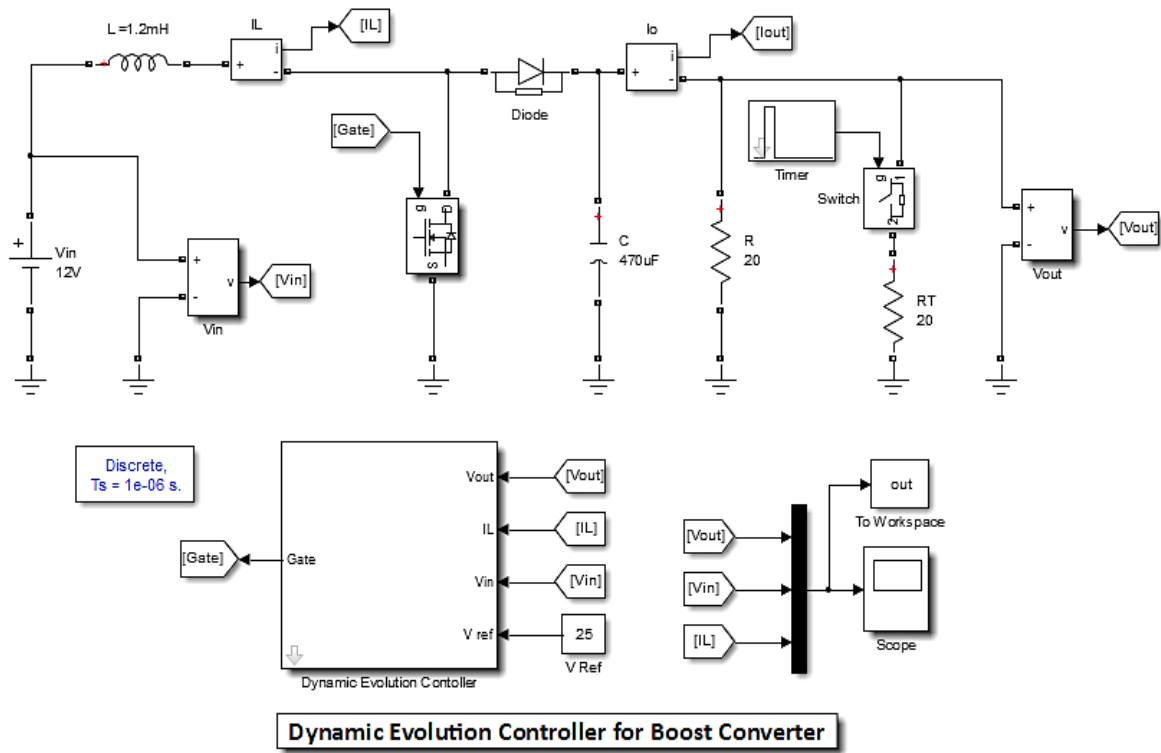


Figure 4. Model of boost converter system using dynamic evolution control

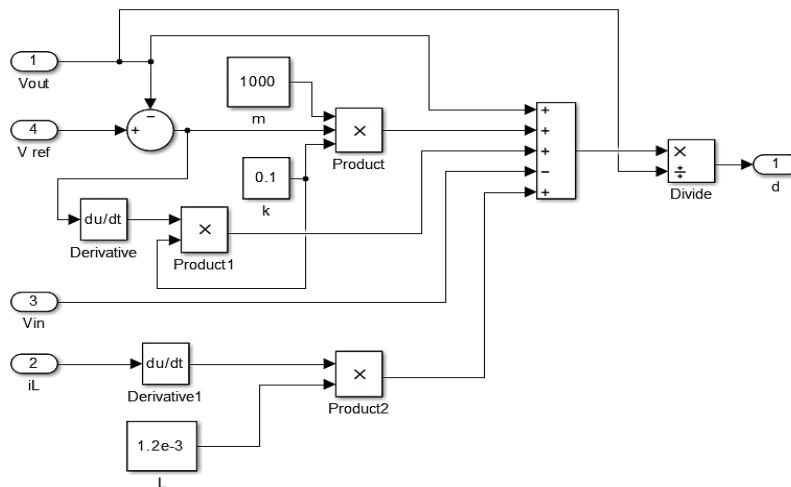


Figure 5. Model of dynamic evolution controller

Figure 7 illustrates the simulation results for the boost converter’s output voltage with V_{in} set at 16 V. Just as in the previous case, the controllers effectively regulate the output voltage to 25 V. This configuration yields an average duty cycle of 36%. The output current remains at 1.25 A, and the estimated input current amounts to 1.95 A.

Figure 8 showcases the simulation results of the boost converter’s output voltage with V_{in} set at 20 V. Similar to the previous scenarios, the controllers maintain the output voltage at 25 V when given a reference voltage of 25 V. The average duty cycle equals 20%. The output current remains consistent at 1.25 A. The estimated input current is approximately 1.56 A. To assess the DEC controller’s capability to manage variations in the load, simulations were conducted involving load resistance changes from 20 ohms to 10 ohms. Figure 9 displays the output voltage, input voltage, and inductor current while transitioning the load from 20 ohms to 10 ohms, with V_{in} set at 12 V and V_{ref} at 25 V.

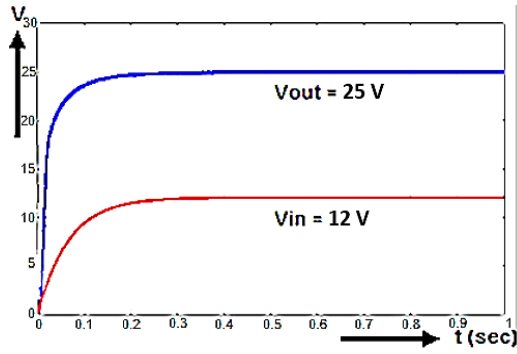


Figure 6. Boost converter output voltage with $V_{in} = 12\text{ V}$

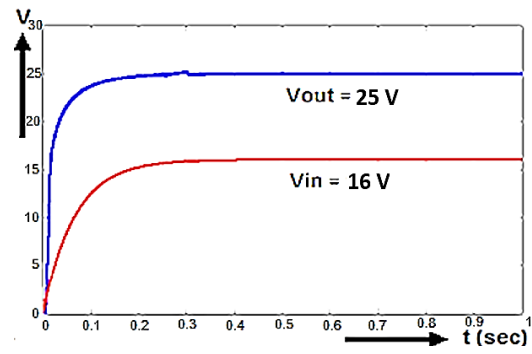


Figure 7. Boost converter output voltage with $V_{in} = 16\text{ V}$

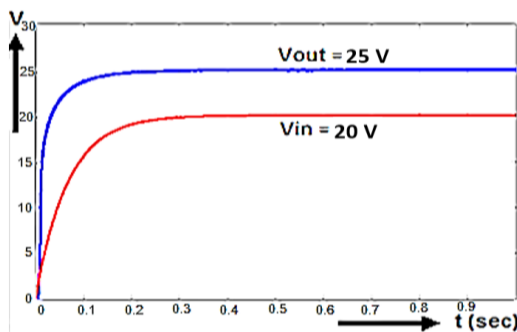


Figure 8. Boost converter output voltage with $V_{in} = 20\text{ V}$

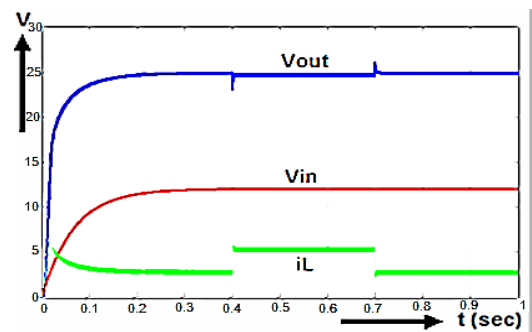


Figure 9. Output voltage, input voltage and i_L current

3.2. Hardware result

To validate the effectiveness of dynamic evolution control in controlling the boost DC-DC converter, a hardware prototype was developed. Figure 10 illustrates the schematic of the boost converter prototype, which encompasses three main circuit part. The first part is the power circuit, constructed using components such as the IRFP4110 power MOSFET, an ultrafast 60EPU04P diode, a 1.2 mH power inductor, and a 470 uF electrolytic capacitor. The second part constitutes the gate drive circuit, which is designed with the TLP250 IC. The third part is the controller circuit, with the Atmega328P microcontroller serving as the main controller. This microcontroller is a high-performance, low-power 8-bit AVR microcontroller with up to 16 MIPS throughput at 16 MHz, two 8-bit Timers/Counters, one 16-bit Timer/Counter with separate prescaler, 6 PWM channels, and 8 10-bit ADCs channel. The complete boost converter hardware prototype is depicted in Figure 11.

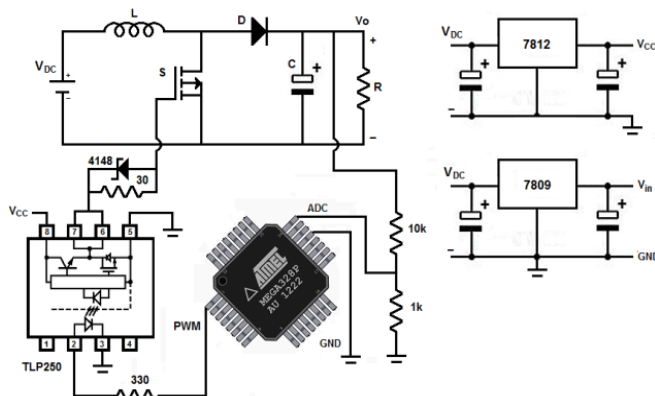


Figure 10. The schematic of boost converter proptotype

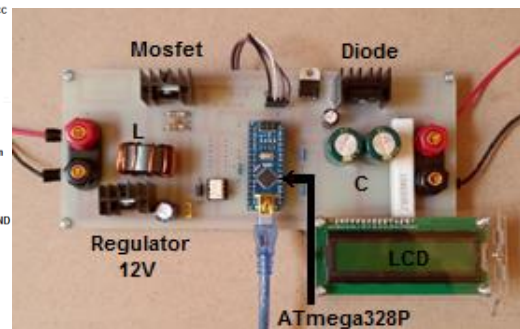


Figure 11. Hardware prototype of boost DC-DC converter

3.3. Effect of parameters m and k on dynamic evolution control

The experimental study involved hardware implementation of the boost converter controlled by dynamic evolution control. Figures 12 and 13 depict the output voltage waveforms of the boost converter when subjected to dynamic evolution control. To analyze the impact of parameters m and k on the performance of dynamic evolution control, this study examined the k parameter, considering values of 0.1 and 0.25, and varied the parameter m accordingly. Figures 12(a) to 12(d) showcase the boost converter's output voltage under dynamic evolution control with $k = 0.1$ and m values of 1000, 2000, 3000, and 5000, respectively. Similarly, Figures 13(a) to 13(d) display the boost converter's output voltage with $k = 0.25$ and m values of 1000, 2000, 3000, and 5000, respectively.

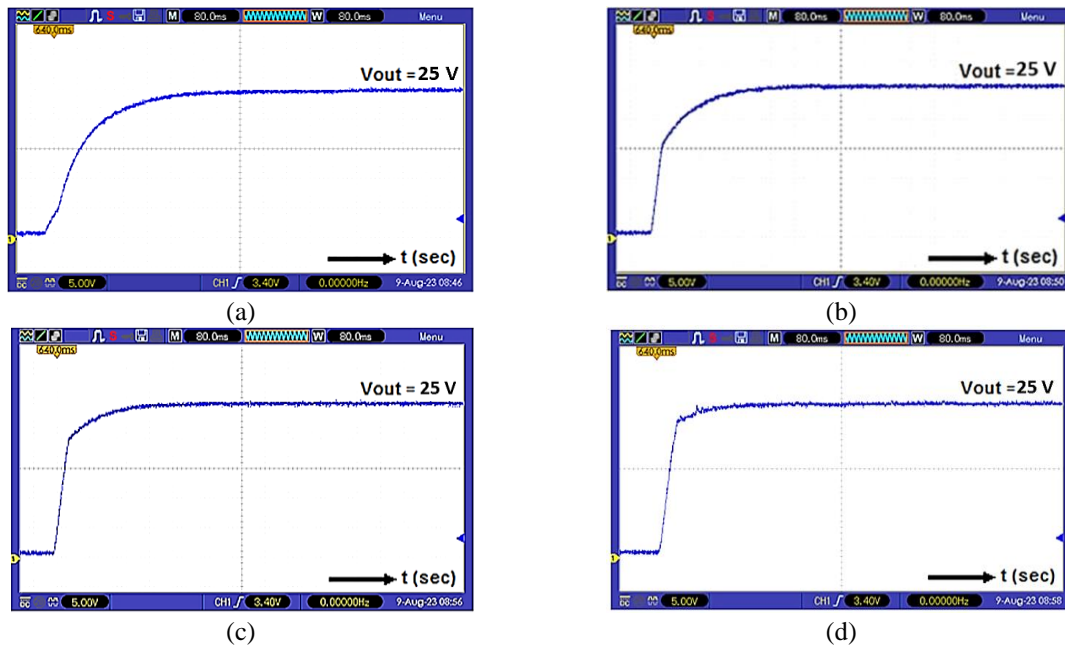


Figure 12. Output voltage of boost converter using dynamic evolution control with $k = 0.1$:
(a) $m = 1000$, (b) $m = 2000$, (c) $m = 3000$, and (d) $m = 5000$

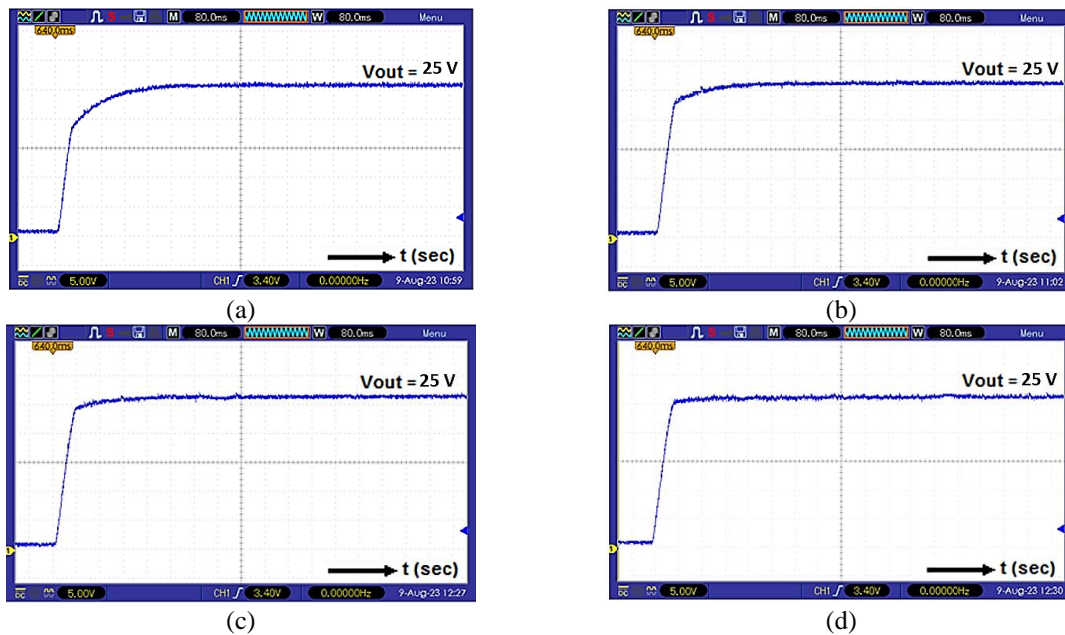


Figure 13. Output voltage boost converter using dynamic evolution control with $k=0.25$:
(a) $m=1000$, (b) $m=2000$, (c) $m=3000$, and (d) $m=5000$

With a constant 12 V input and a 25 V reference setting, the boost converter consistently produces an output voltage very close to the reference value. There's no overshooting, and the initial output waveform is similar to the typical dynamic evolution control output pattern shown in Figure 3(b). In Figures 12 and 13, it's evident that higher m values result in faster dynamic evolution control responses. For instance, when using $k = 0.1$ and $m = 2000$, the boost converter's output voltage stabilizes within just 160 milliseconds, with ripple voltage of 0.2 V. These results highlight the precision and effectiveness of the proposed dynamic evolution control technique for regulating the boost converter's output voltage.

3.4. Variable input voltage test

In this experiment, the boost converter was tested under dynamic evolution control using various input voltages: 12 V, 16 V, and 20 V, while the reference voltage remained fixed at 25 V. The experimental results confirm that the dynamic evolution control effectively regulates the boost converter, producing an output voltage closely aligned with the set reference voltage. Hardware results are presented in Figure 14, Figure 15, and Figure 16.

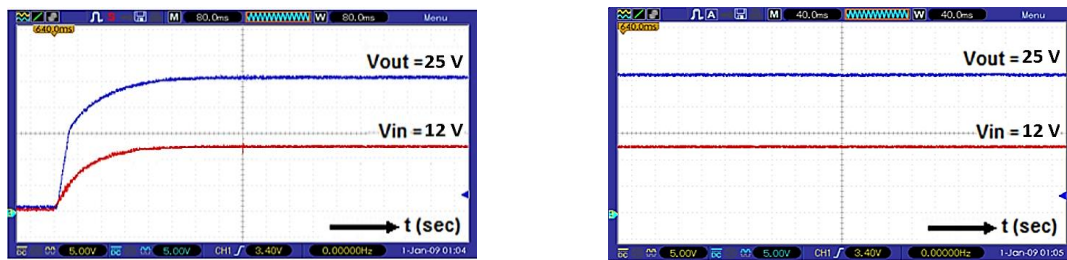


Figure 14. Boost converter input and output voltage with $V_{in} = 12$ V

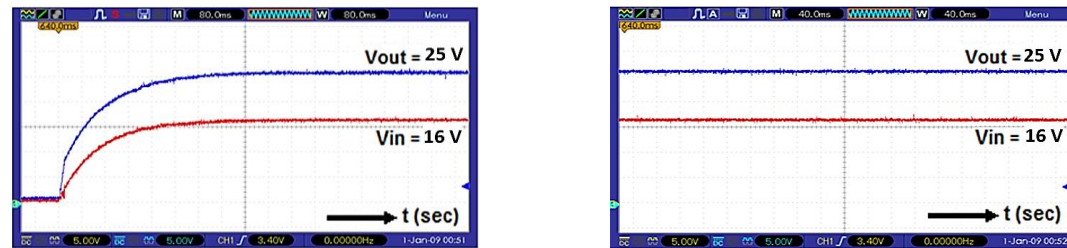


Figure 15. Boost converter input and output voltage with $V_{in} = 16$ V

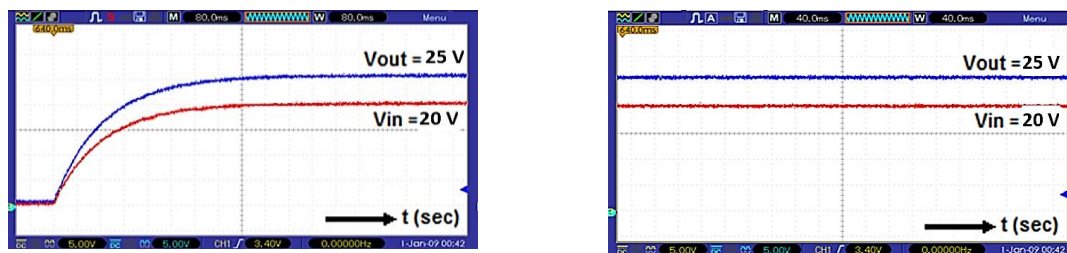


Figure 16. Boost converter input and output voltage with $V_{in} = 20$ V

4. CONCLUSION

This paper presents the design and hardware implementation of a dynamic evolution control for a boost converter. The implementation of the controller, which is based on the dynamic evolution control theory, is achieved by utilizing the ATmega328P microcontroller. The investigation of the performance of the DC-DC boost controller system utilizing dynamic evolution control has been conducted under conditions of varying input voltage. The findings from the simulation results and hardware experiments demonstrate that dynamic evolution control exhibits a high degree of efficacy in regulating the boost converter, effectively ensuring the maintenance of the desired output voltage level.

ACKNOWLEDGEMENTS

The authors wish to extend their appreciation to the University of Lampung for furnishing research amenities. The study received backing from the Fundamental Research Funding administered by the Directorate General of Higher Education, Research, and Technology under the Ministry of Education, Culture, Research, and Technology of the Republic of Indonesia.




REFERENCES

- [1] Z. Zhao and X. He, "Research on Digital Synchronous Rectification for a High-Efficiency DC-DC Converter in an Auxiliary Power Supply System of Magnetic Levitation," *Energies*, vol. 13, no. 1, p. 51, Dec. 2019, doi: 10.3390/en13010051.
- [2] M. A. N. Amran, A. A. Bakar, M. H. A. Jalil, A. F. H. A. Gani, and E. Pathan, "Optimal tuning of proportional-integral controller using system identification for two-phase boost converter for low-voltage applications," *Int. J. Power Electron. Drive Syst.*, vol. 12, no. 4, pp. 2393–2402, 2021, doi: 10.11591/ijpeds.v12.i4.pp2393-2402.
- [3] F. Jin, A. Nabih, C. Chen, X. Chen, Q. Li, and F. C. Lee, "A High Efficiency High Density DC/DC Converter for Battery Charger Applications," in *2021 IEEE Applied Power Electronics Conference and Exposition (APEC)*, Jun. 2021, pp. 1767–1774. doi: 10.1109/APEC42165.2021.9487108.
- [4] A. Bilsalam, N. Bizon, and P. Thounthong, "Improved auxiliary inductive coil connectors in DC boost converters with high voltage gain for renewable energy source applications," *Int. J. Power Electron. Drive Syst.*, vol. 13, no. 3, pp. 1498–1509, 2022, doi: 10.11591/ijpeds.v13.i3.pp1498-1509.
- [5] K. Mahalingam and G. Jothimani, "An elevated gain DC-DC converter with active switched inductor for PV application," *Int. J. Power Electron. Drive Syst.*, vol. 14, no. 2, pp. 892–897, 2023, doi: 10.11591/ijpeds.v14.i2.pp892-897.
- [6] A. D. G. Jegha, M. S. P. Subathra, N. M. Kumar, U. Subramaniam, and S. Padmanaban, "A high gain DC-DC converter with grey wolf optimizer based MPPT algorithm for PV fed BLDC motor drive," *Appl. Sci.*, vol. 10, no. 8, 2020, doi: 10.3390/AP10082797.
- [7] R. K. Dasari and D. G. Immanuel, "Photovoltaic hybrid boost converter fed switched reluctance motor drive," *Int. J. Power Electron. Drive Syst.*, vol. 13, no. 1, pp. 275–288, 2022, doi: 10.11591/ijpeds.v13.i1.pp275-288.
- [8] S. Srinivasan, R. Tiwari, M. Krishnamoorthy, M. P. Lalitha, and K. K. Raj, "Neural network based MPPT control with reconfigured quadratic boost converter for fuel cell application," *Int. J. Hydrogen Energy*, vol. 46, no. 9, pp. 6709–6719, 2021, doi: 10.1016/j.ijhydene.2020.11.121.
- [9] R. H. Mohammed, A. A. Abdulrazzaq, and W. K. Al-Azzawi, "Benefits of MPP tracking PV system using perturb and observe technique with boost converter," *Int. J. Power Electron. Drive Syst.*, vol. 13, no. 4, pp. 2468–2477, 2022, doi: 10.11591/ijpeds.v13.i4.pp2468-2477.
- [10] B. T. Kadhem, S. S. Harden, O. Y. K. Al-Atbee, and K. M. Abdulhassan, "Improve the energy efficiency of PV systems by installing a soft switching boost converter with MPPT control," *Int. J. Power Electron. Drive Syst.*, vol. 14, no. 2, pp. 1055–1069, 2023, doi: 10.11591/ijpeds.v14.i2.pp1055-1069.
- [11] P. S. Kumar, R. P. S. Chandrasena, V. Ramu, G. N. Srinivas, and K. V. S. M. Babu, "Energy Management System for Small Scale Hybrid Wind Solar Battery Based Microgrid," *IEEE Access*, vol. 8, pp. 8336–8345, 2020, doi: 10.1109/ACCESS.2020.2964052.
- [12] A. Zentani, A. Almaktoof, and M. T. E. Kahn, "DC-DC Boost Converter with PO MPPT Applied to a Stand-Alone Small Wind Turbine System," *Proc. - 30th South. African Univ. Power Eng. Conf. SAUPEC 2022*, 2022, doi: 10.1109/SAUPEC55179.2022.9730744.
- [13] A. F. Murtaza, H. A. Sher, F. Usman Khan, A. Nasir, and F. Spertino, "Efficient MPP Tracking of Photovoltaic (PV) Array Through Modified Boost Converter With Simple SMC Voltage Regulator," *IEEE Trans. Sustain. Energy*, vol. 13, no. 3, pp. 1790–1801, 2022, doi: 10.1109/TSTE.2022.3172315.
- [14] R. S. Inomoto, J. R. B. A. Monteiro, and A. J. Sguarezi Filho, "Boost Converter Control of PV System Using Sliding Mode Control With Integrative Sliding Surface," *IEEE J. Emerg. Sel. Top. Power Electron.*, 2022, doi: 10.1109/JESTPE.2022.3158247.
- [15] N. H. Baharudin, T. M. N. T. Mansur, F. A. Hamid, R. Ali, and M. I. Misrun, "Topologies of DC-DC converter in solar PV applications," *Indones. J. Electr. Eng. Comput. Sci.*, vol. 8, no. 2, pp. 368–374, 2017, doi: 10.11591/ijeecs.v8.i2.pp368-374.
- [16] A. S. Samosir, S. Purwiyanti, H. Gusmedi, and M. Susanto, "Design of DC to DC Converter for Solar Photovoltaic Power Plant Applications," *Proc. - ICCTEIE 2021 2021 Int. Conf. Converging Technol. Electr. Inf. Eng. Converging Technol. Sustain. Soc.*, pp. 132–137, 2021, doi: 10.1109/ICCTEIE54047.2021.9650639.
- [17] B. Sri Revathi and M. Prabhakar, "Non isolated high gain DC-DC converter topologies for PV applications – A comprehensive review," *Renew. Sustain. Energy Rev.*, vol. 66, pp. 920–933, 2016, doi: 10.1016/j.rser.2016.08.057.
- [18] M. Z. Hossain, N. A. Rahim, and J. a/l Selvaraj, "Recent progress and development on power DC-DC converter topology, control, design and applications: A review," *Renew. Sustain. Energy Rev.*, vol. 81, pp. 205–230, 2018, doi: 10.1016/j.rser.2017.07.017.
- [19] A. S. Samosir and A. H. M. Yatim, "Dynamic evolution control for synchronous buck DC–DC converter: Theory, model and simulation," *Simul. Model. Pract. Theory*, vol. 18, no. 5, pp. 663–676, May 2010, doi: 10.1016/j.simpat.2010.01.010.
- [20] C. Yanarates and Z. Zhou, "Design and Cascade PI Controller-Based Robust Model Reference Adaptive Control of DC-DC Boost Converter," *IEEE Access*, vol. 10, pp. 44909–44922, 2022, doi: 10.1109/ACCESS.2022.3169591.
- [21] B. A. Martinez-Trevino, A. El Aroudi, A. Cid-Pastor, and L. Martinez-Salamero, "Nonlinear control for output voltage regulation of a boost converter with a constant power load," *IEEE Trans. Power Electron.*, vol. 34, no. 11, pp. 10381–10385, 2019, doi: 10.1109/TPEL.2019.2913570.
- [22] H. B. Yuan and Y. B. Kim, "Compensated active disturbance rejection control for voltage regulation of a DC–DC boost converter," *IET Power Electron.*, vol. 14, no. 2, pp. 432–441, 2021, doi: 10.1049/pe12.12049.
- [23] K. Aseem and S. Selva Kumar, "Closed loop control of dc-dc converters using pid and fopid controllers," *Int. J. Power Electron. Drive Syst.*, vol. 11, no. 3, pp. 1323–1332, 2020, doi: 10.11591/ijpeds.v11.i3.pp1323-1332.
- [24] H. K. Khleaf, A. K. Nahar, and A. S. Jabbar, "Intelligent control of DC-DC converter based on PID-neural network," *Int. J. Power Electron. Drive Syst.*, vol. 10, no. 4, pp. 2254–2262, 2019, doi: 10.11591/ijpeds.v10.i4.pp2254-2262.
- [25] H. Attia, "Improved Boost Converter by Utilizing Sliding Mode Control; Comparative Study," *2022 Int. Conf. Electr. Comput. Technol. Appl. ICECTA 2022*, pp. 68–71, 2022, doi: 10.1109/ICECTA57148.2022.9990353.
- [26] S. Abboud, R. Habachi, A. Boulal, and S. El Alami, "Maximum power point tracker using an intelligent sliding mode controller of a photovoltaic system," *Int. J. Power Electron. Drive Syst.*, vol. 14, no. 1, pp. 516–524, 2023, doi: 10.11591/ijpeds.v14.i1.pp516-524.
- [27] Z. Wang, S. Li, and Q. Li, "Continuous nonsingular terminal sliding mode control of dc-dc boost converters subject to time-varying disturbances," *IEEE Trans. Circuits Syst. II Express Briefs*, vol. 67, no. 11, pp. 2552–2556, 2020, doi: 10.1109/TCSII.2019.2955711.




- [28] L. Ardhenta and T. Nurwati, "Comparison of sliding mode controller application for buck-boost converter based on linear sliding surface," *Int. J. Power Electron. Drive Syst.*, vol. 13, no. 1, pp. 423–431, 2022, doi: 10.11591/ijpeds.v13.i1.pp423-431.
- [29] S. Ahmad and A. Ali, "Unified Disturbance-Estimation-Based Control and Equivalence with IMC and PID: Case Study on a DC-DC Boost Converter," *IEEE Trans. Ind. Electron.*, vol. 68, no. 6, pp. 5122–5132, 2021, doi: 10.1109/TIE.2020.2987269.
- [30] K. G. Shankar, D. Jena, and R. Reddivari, "Comparative Overview of Internal Model Control Based PID, State Feedback Integral, and Sliding Mode Controllers for Buck Converter," *2019 IEEE Int. Conf. Distrib. Comput. VLSI, Electr. Circuits Robot. Discov. 2019 - Proc.*, 2019, doi: 10.1109/DISCOVER47552.2019.9008056.

BIOGRAPHIES OF AUTHORS






Ahmad Saudi Samosir    is a lecturer in Electrical Engineering Department at the Universitas Lampung, Lampung, Indonesia. He received his B.Eng., M.Eng. and Ph.D. degrees in in Electrical Engineering from Universitas Sumatera Utara, Institut Teknologi Bandung and Universiti Teknologi Malaysia, in 1995, 1999 and 2010, respectively. He has been a Professor in Universitas Lampung Indonesia since 2017. His research interests include power electronics design, controller and its applications in renewable energy, electric vehicle and industrial applications. He can be contacted at email: ahmad.saudi@eng.unila.ac.id.






Sri Ratna Sulistiyanti    is a lecturer in Electrical Engineering Department at the Universitas Lampung, Lampung, Indonesia. She received her M.Eng. and Dr. degrees in Electrical Engineering Gadjah Mada University, Indonesia, in 2000 and 2011, respectively. She is currently a lecturer of Universitas Lampung. Her research interests include instrumentation electronic, image processing, thermal imaging, and controller and its applications in renewable energy, electric vehicle and industrial applications. She can be contacted at email: sr_sulistiyanti@eng.unila.ac.id.



Herri Gusmedi    is a lecturer in Electrical Engineering Department at the Universitas Lampung, Lampung, Indonesia. He received his B.Eng., M.Eng. degree in Electrical Engineering from Universitas Sriwijaya and Institut Teknologi Bandung respectively in 1995, 2000. Served as Head of Electric Power System Laboratory at Universitas Lampung, Indonesia since 2020. His research interests include system reliability design, economical operation, power converter and renewable energy, especially photovoltaic. He can be contacted at email: herri.gusmedi@eng.unila.ac.id.



Luthfiyyatun Mardiyah    is a fresh graduate in Electrical Engineering Department at the Universitas Lampung, Lampung, Indonesia. She received her B.Eng. in 2022. She is currently pursuing her Master degree in Electrical Engineering at Universitas Diponegoro. Her research interests include power electronics, controller, and its applications. She can be contacted at email: luthfi.mardiah@gmail.com.